Comparative Study of Microcelluloses Isolated From Two Different Biomasses with Commercial Cellulose

Wei Tieng Owi,[a] Ong Hui Lin,[a,*] Sung Ting Sam,[b] Chin Hua Chia,[c] Sarani Zakaria,[c] Muhammad Safwan Mohaiyiddin,[a] Al Rey Villagracia,[d] Gil Nonato Santos,[d] and Hazizan Md Akil [e]

Microcelluloses (MCs) were chemically isolated from two different biomass sources, empty fruit bunches (EFB) and sugarcane bagasse (SCB). The resulting MCs were compared to the commercially available cellulose (MC-Sigma) that was used as a standard. Structural, crystalline, morphological, and thermal properties of all specimens were characterized and compared by Fourier transform infrared (FTIR) spectroscopy, X-ray diffraction (XRD), scanning electron microscopy (SEM), thermogravimetric analysis (TGA), and differential scanning calorimetry (DSC). FTIR analysis verified that the chemical treatments removed non-cellulosic constituents including hemicelluloses and lignin. XRD patterns revealed the crystallinity increment from 43.1% to 52.1% for MC-EFB and 38.9% to 52.4% for MC-SCB. SEM images demonstrated the fibrillar structure of both MC-EFB and MC-SCB, and their surfaces were smoother compared with MC-Sigma. From the TG curves, MC-EFB provided the highest thermal stability, as it had the highest maximum degradation temperature at 345 °C. DSC results showed only one endothermic peak for all specimens. Taken together, these results reasonably confirmed that the MCs from EFB and SCB are comparable to standard MC-Sigma.

Keywords: Empty fruit bunches; Characterization; Microcellulose; Sugarcane bagasse

*Contact information: a: School of Materials Engineering, Universiti Malaysia Perlis, 02600 Arau, Perlis, Malaysia; b: School of Bioprocess Engineering, Universiti Malaysia Perlis, 02600 Arau, Perlis, Malaysia; c: School of Applied Physics, Faculty of Science and Technology, Universiti Kebangsaan Malaysia, 43600 Bangi, Selangor, Malaysia; d: Physics Department, College of Science, De La Salle University, 2401 Taft Avenue, Manila 1004, Philippines; e: School of Materials and Mineral Resources Engineering, Universiti Sains Malaysia, 14300 Nibong Tebal, Penang, Malaysia; *Corresponding author: hlong@unimap.edu.my*

INTRODUCTION

Cellulose is the most abundant renewable polymer on the Earth (Siqueira *et al.* 2010; Salas *et al*. 2014), and it is one of the most crucial natural polymers present in the biosphere (Brinchi *et al.* 2013). Cellulose has attracted a lot of attention due to its excellent properties, such as biocompatibility, biodegradability, and thermal and chemical stability (Tsioptsias *et al.* 2008; Chen *et al.* 2015a). This natural hydrophilic polymer is composed of polymer chains made of unbranched β (1,4) linked D-glucopyranosyl units, and the length of these β (1,4) glucan chains depends on the origin of the cellulose (Abdul Khalil *et al.* 2012). Cellulose is a very strong natural polymer, as shown by the fact that it is the building component of long fibrous cells, and it has been extensively applied in the paper, textile, food, and coating industries (Edgar *et al*. 2001; Azeredo 2009). Major sources of cellulose are cotton (Morais *et al*. 2013), jute (Jahan *et al*. 2011), wood (Abe *et al*. 2007; Mikhailidi *et al*. 2014), hemp (Wang *et al.* 2007), soy hulls (Alemdar and Sain 2008),

pineapple leaf (Cherian *et al*. 2010; Santos *et al*. 2013), rice husk (Johar *et al.* 2012), mengkuang leaves (Sheltami *et al*. 2012), and empty fruit bunches (Sharma *et al.* 2015).

At present, microcellulose (MC) is used in different fields such as pharmacy, cosmetics, personal care, and the food industry. For dietary purposes, MC powder is used as a filler and binder in medical tablets and food tablets (Adel *et al*. 2011), while the gel form is used as a viscosity regulator, suspending agent, and an emulsifier in various pastes and creams (Laka and Chernyavskaya 2007). The promising performance of MC in various applications has stimulated the utilization of biomasses that supply cellulose, for instance, empty fruit bunches (EFB) and sugarcane bagasse (SCB) (Cherian *et al*. 2010).

The oil palm tree *Elaeis guineensis* is an agricultural plant and a vital crop that contributes to the economic growth of Malaysia. A total biomass of 95 million tons is generated annually, and its lignocellulosic constituents supplies the new industry of oil palm biomass, which produces fertilizer, animal feed, composite material, and pulp (Lamaming *et al*. 2015). Oil palm bio-fiber waste, such as EFB, is a lignocellulosic material that consists of approximately 44.2% cellulose, 33.5% hemicellulose, and 20.4% lignin (Hamzah *et al.* 2011). Thus, EFB can be employed as a raw fiber for the isolation of MC.

Sugarcane bagasse is another lignocellulosic biomass which is naturally low-cost, locally available, and rich in cellulose. It is the fibrous by-product obtained after sugarcane stalks are crushed for juice extraction (Faruk *et al*. 2012; Slavutsky and Bertuzzi 2014). Similar to EFB, SCB is comprised of 40% cellulose, 24% hemicellulose, and 25% lignin (Noor Hasyierah *et al*. 2008).

In previous studies, there have been many comparisons and exploitations made for cellulose from various types of plants (Das *et al.* 2010; Virtanen *et al*. 2012; Chen *et al*. 2015b). However, there have not been any comparisons of the characteristics of MC obtained from different biomasses, such as EFB and SCB. In this study, EFB and SCB were selected as two different biomasses that provided raw fibers for MC isolation using chemical treatments. The resultant MC was characterized using Fourier transform infrared (FTIR) spectroscopy, X-ray diffraction (XRD), scanning electron microscopy (SEM), thermogravimetric analysis (TGA), and differential scanning calorimetry (DSC). These properties were compared to a commercial cellulose standard.

EXPERIMENTAL

Materials

Empty fruit bunches were collected at United Oil Palm Industries Sdn. Bhd, Nibong Tebal, Malaysia, and sugarcane bagasse was collected from a local food stall in Perlis, Malaysia. The commercial microcrystalline cellulose, 20 µm in size, was purchased from Sigma Aldrich (Germany). Sodium hydroxide (NaOH) and acetic acid glacial were obtained from HmbG Chemicals (Germany); sodium chlorite ($NaClO_2$) was supplied by Acros (Belgium). All chemicals were used as supplied by the manufacturer.

Methods

Preparation of EFB and SCB specimens prior to cellulose isolation

EFB were washed and soaked with clean water to remove impurities from fiber surfaces, such as oil and sand particles, until the wash water remained colorless. SCB was peeled off to obtain its white portion, which was rinsed until the water was no longer

cloudy. EFB and SCB were dried in oven at 60 °C for 24 h and cut into 0.5- to 1-cm segments. The cut fibers were ground and passed through a 100 sieve mesh (150 µm).

Isolation of cellulose

Ground fibers from EFB (40 g) and SCB (20 g) were first alkaline treated in 800 mL of 4 wt% NaOH solution to remove hemicelluloses. For delignification, alkaline-treated fibers were bleached with 1.7 wt% $NaClO_2$ solution in an acetic acid buffer (40 g of NaOH pellets, 75 mL glacial acetic acid, and 925 mL distilled water) in a 1000-mL volumetric flask. Equal volumes of fibers in distilled water, 1.7 wt% of $NaClO_2$ solution, and acetic acid buffer were mixed to a total volume of 800 mL. Both treatments were conducted at 80 °C for 2 h with constant stirring. The treated fibers were strained and washed using cloth filters and distilled water until the pH reached 7. Alkaline treatment and fiber bleaching were repeated 3 times to isolate white MC. MC isolated from EFB was denoted as MC-EFB, and MC isolated from SCB was denoted as MC-SCB. Commercial cellulose was denoted as MC-Sigma.

Characterization

Fourier transform infrared spectroscopy

The functional groups of the cellulosic specimens were analyzed with a Spectrum RX FTIR spectrophotometer (Perkin Elmer, USA). The dried powder specimens were mixed with potassium bromide (KBr) with a ratio of 1:99 (%) and homogenized using a mortar and pestle. The mixture was compressed into ultrathin pellets at a pressure of 10 ton for 2 min. FTIR spectra were recorded in the range of 4000 to 500 cm^{-1} with 32 scans and a resolution of 4 cm^{-1}.

X-ray diffraction

The XRD patterns were investigated using a Desktop D2 Phaser X-ray diffractometer (Bruker Corporation, USA) with CuKα radiation operating at 30 kV and 10 mA. The specimens were filled compactly into the plastic specimen holder with a diameter of 2.5 cm and a thickness of 0.1 cm before testing. Data were collected at 2θ angles between 10 to 30° with a scan rate of 2 °/s. The crystallinity index (CI) can be calculated either by the XRD peak height method (Mtibe *et al*. 2015) or the deconvolution method (Segal *et al*. 1959). In this study, CI was determined by deconvolution method and calculated using Eq. 1 as shown below,

$$CI = [(I_{002} - I_{AM}) / I_{002}] \times 100\% \quad (1)$$

where I_{002} is the highest peak intensity for the crystalline region and I_{AM} is the minimum peak intensity for the amorphous region. I_{002} represents both the crystalline and amorphous materials, while I_{AM} represents just the amorphous material

Scanning electron microscopy

Morphological characteristics of the specimens were observed with a JSM-6460 LA SEM (JEOL Ltd., Japan) with an accelerated voltage of 5 kV. Prior to examination, the specimens were mounted on the specimen holders using double-sided tape and coated with platinum using a JEOL JFC-1600 Auto Fine Coater.

Thermogravimetric analysis

A Pyris Diamond TG/DTA instrument (Perkin Elmer, USA) was used to measure the thermal stability of raw materials and the three MCs from different sources. Approximately 10 mg of each specimen was heated at a rate of 10 °/min from 30 to 800 °C under nitrogen gas flow of 20 mL/min using a ceramic pan.

Differential scanning calorimetry

A DSC Q10 instrument (TA Instruments, USA) was used to study the thermal behavior of the specimens. Approximately 10 mg of each specimen was heated from 30 to 200 °C at a heating rate of 10 °C/min using an aluminum pan. The testing was performed under a nitrogen gas atmosphere with a flow rate of 20 mL/min.

RESULTS AND DISCUSSION

Fourier Transform Infrared Spectroscopy

Figure 1 compares the FTIR spectra between each raw fiber and its resultant MC, and Fig. 2 displays the FTIR spectra of MC from EFB, SCB, and Sigma. In general, the spectra for raw EFB and raw SCB were identical. The spectral bands located at 3,400 to 3,340 cm^{-1} and 2,923 to 2,906 cm^{-1} were found in all the spectra and represented the O-H stretching of intermolecular hydrogen bonds and aliphatic saturated C-H stretching, respectively. The hydroxyl group represented in the first spectral band is related to the moisture content, where OH is bonded to the structure of cellulose, hemicellulose, and lignin. The peaks at 1,735 cm^{-1} for raw EFB and 1,740 cm^{-1} for SCB were assigned to the acetyl and ester groups in hemicellulose and in aromatic components of lignin (De Rosa *et al*. 2010). These peaks disappeared in the MC spectra. The peak at 1,640 cm^{-1} may be attributed to the OH bending mode of adsorbed water (Le Troedec *et al*. 2008). The spectral band at 1,508 to 1,513 cm^{-1} for raw fibers corresponded to C-C stretching vibrations in the lignin aromatic ring, and the peak from 1,248 to 1,255 cm^{-1} (C-O out of plane stretching because of aryl group in lignin) was associated with the chemical treatments.

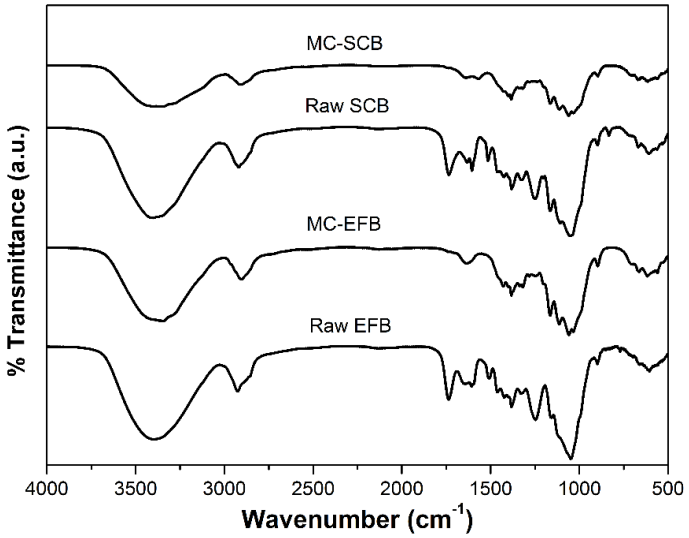

Fig. 1. FTIR spectra of Raw EFB, MC-EFB, Raw SCB, and MC-SCB

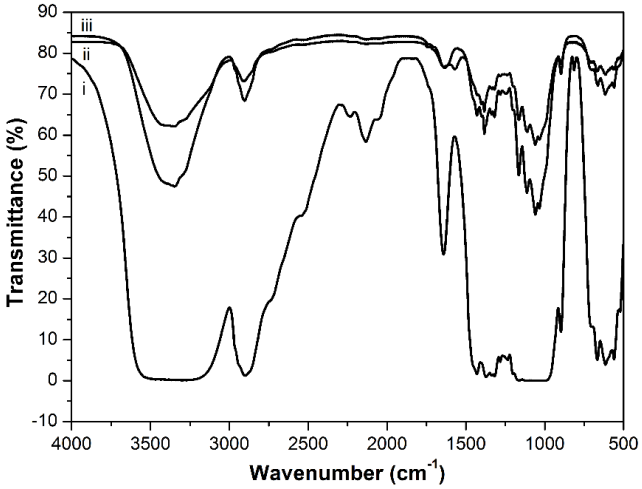

Fig. 2. FTIR spectra of (i) MC-Sigma, (ii) MC-SCB, and (iii) MC-EFB

The effectiveness of the chemical treatments was revealed through these two main spectral bands, such that the band at 1,508 to 1,513 cm^{-1} is absent and the band at 1,248 to 1,255 cm^{-1} is reduced drastically (Kumar *et al*. 2012). The peak at 899 cm^{-1} in all spectra may be the β-glycosidic linkages of glucose rings in cellulose (Kaushik *et al*. 2010). Overall, the FTIR spectra demonstrated that MC was successfully isolated from EFB and SCB by chemical treatments, and nearly all of the MC-EFB and MC-SCB peaks were similar to those of MC-Sigma. However, a few peaks were broader in the MC-Sigma spectrum, especially the peak at 3,353 cm^{-1}, which were due to the moisture content. This result suggested that MC-Sigma absorbs more moisture than MC-EFB and MC-SCB.

X-ray Diffraction Studies

The XRD profiles of raw EFB, raw SCB, MC-EFB, MC-SCB, and MC-Sigma revealed two well-defined peaks of cellulose at around $2\theta = 15°$ (for the 001 peak) and $2\theta = 22.5°$ (for the 002 peak) (Fig. 3). These diffractograms are typical of semi-crystalline substances with crystalline peaks and amorphous broad hump (Santos *et al*. 2013).The reflection peak at $2\theta = 22.5°$ in raw fibers was more intense after chemical treatments, which corroborated the FTIR analysis. The increased peak intensity could be due to the fact that the raw fibers contain non-cellulosic amorphous materials such as hemicellulose and lignin (Silvério *et al*. 2013; Mtibe *et al.* 2015). The higher crystallinity values of MC-EFB and MC-SCB compared to raw were due to the reduction and removal of non-cellulosic compounds triggered by alkaline treatment and bleaching process (Neto *et al*. 2013). Moreover, the combination of low concentration of sodium hydroxide with low processing temperature could not alter the structure of cellulose, as demonstrated by XRD diffractograms (Chan *et al*. 2013). Although raw SCB showed the lowest crystallinity index (CI) yet the CI of MC-SCB was almost identical and even higher compared to MC-EFB (Table 1). The highest CI was 65.2% for MC-Sigma, followed by MC-SCB and MC-EFB, which were found to be 52.4% and 52.1%, respectively. The CI of both isolated MC-SCB and MC-EFB are nearly equivalent to the value of 54% for cellulose from pineapple leaf fibers, which was reported by Cherian *et al*. (2010). However, it is lower than the 69.5% reported for extracted cellulose from mengkuang leaves or *Pandanus tectorius* by Sheltami *et al*. (2012). Therefore, the CIs of both MCs produced from raw EFB and SCB are comparable to the commercial cellulose MC-Sigma and also some of the celluloses from other natural fibers reported in the literature.

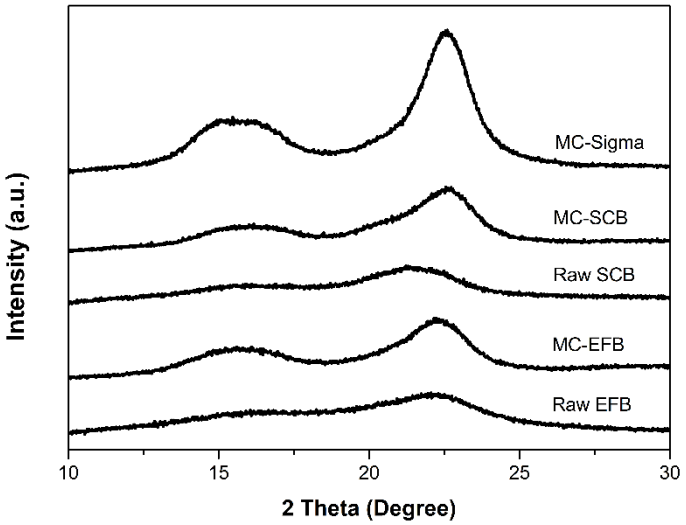

Fig. 3. XRD patterns for all specimens

Table 1. Crystallinity Indices of All Raw Fibers and MCs

Specimen	Crystallinity Index (%)
Raw EFB	43.1
MC-EFB	52.1
Raw SCB	38.9
MC-SCB	52.4
MC-Sigma	65.2

Scanning Electron Microscopy

Morphological structures on the raw fiber surface and their changes after chemical treatments were observed by SEM (Figs. 4, 5). Raw EFB is a lignocellulosic material with compact fibrillar packing, and its external surface showed an irregular heavy deposition of hemicelluloses, lignin, wax, and inorganic components (Fig. 4a; Nazir *et al*. 2013). However, Fig. 4b shows that the surface of raw SCB was smoother than raw EFB, and it also has surface layers full of extractives, such as waxes, pectin, and oil (Kumar *et al*. 2014). The external surface of MC-EFB exhibited a smooth surface with scars, which is possibly due to the removal of hemicellulose, lignin, and inorganic constituents, such as silica (Fig. 5a).

Figure 5b shows that MC-SCB became separated into individual fibers during chemical treatments, resulting in the formation of cellulose fibrillations. Furthermore, the removal of non-cellulosic constituents by chemical treatments cleaved the fibers into smaller sizes (Lu *et al*. 2013). The SEM images of MC-EFB and MC-SCB show the removal of amorphous materials from both raw fibers after chemical treatments, and this observation supports the FTIR and XRD results. Micro-sized cellulose is comprised of strongly hydrogen bonding nanofibers (Chen *et al*. 2011). MC-Sigma had a non-uniform rectangular shape, and the surface was rougher compared with MC-EFB and MC-SCB (Fig. 5c). Although the starting materials were different, the SEM images of MC-EFB and MC-SCB revealed similar morphologies with smoother surfaces than MC-Sigma.

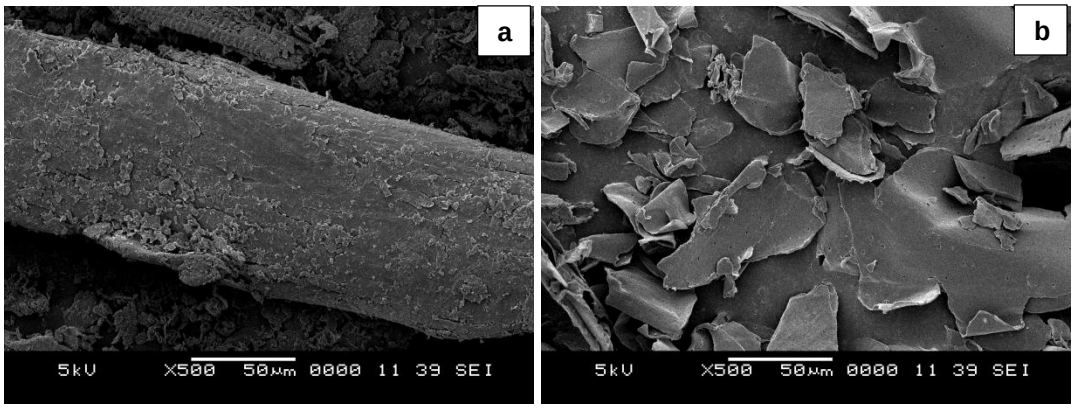

Fig. 4. SEM images of (a) raw EFB and (b) raw SCB

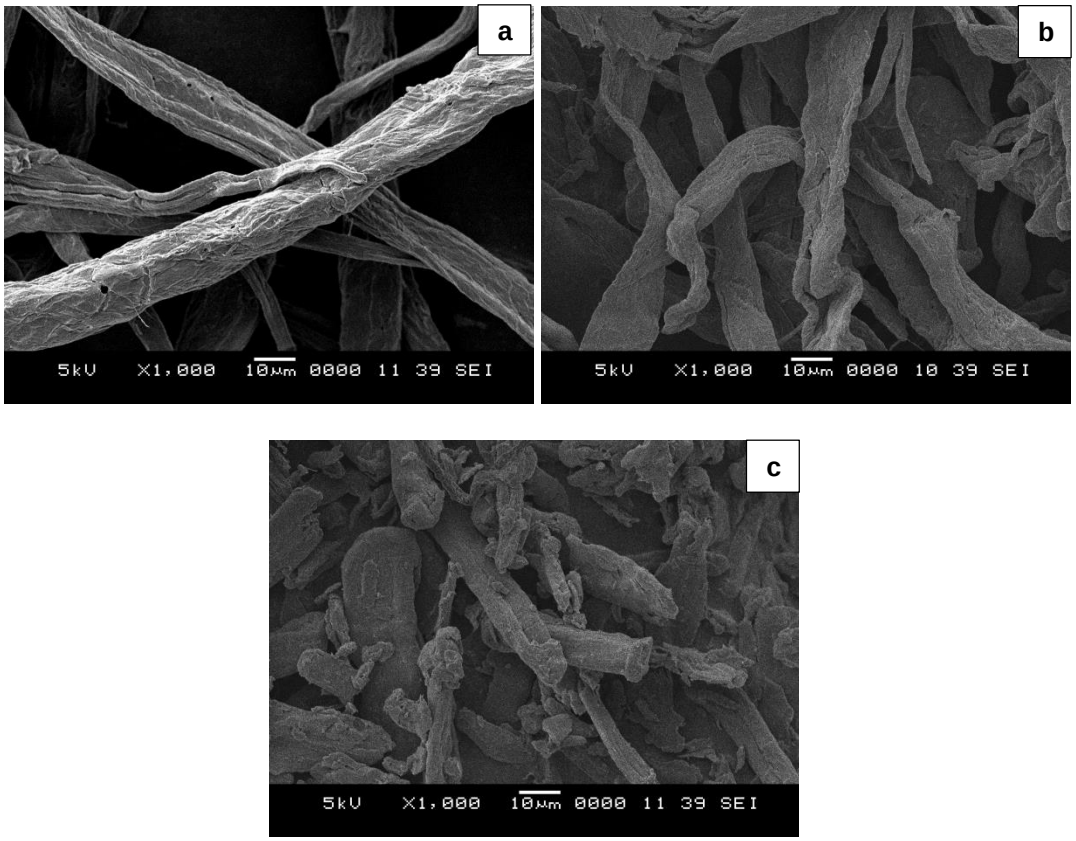

Fig. 5. SEM images of (a) MC-EFB, (b) MC-SCB, and (c) MC-Sigma

Thermogravimetric Analysis

Thermogravimetric analysis elucidates the changes in materials after chemical treatment and also determines the thermal stability of the MCs and raw materials. Understanding the degradation behaviour of materials is crucial to establish their potential applications in biocomposites (Mondragon *et al*. 2014). Figure 6 shows the TGA and derivative thermogravimetry (DTG) curves of all the specimens, including raw fibers and their MCs. There were two weight loss phases in all studied specimens (Fig. 6a); the initial

small weight loss from 30 to 100 °C was due to water vaporization (Rosa *et al*. 2010). Approximately 5% of the specimens absorbed moisture in the initial phase, but the raw EFB and MC-EFB lost approximately 10% of their weight. The second phase weight loss occurred between 200 and 400 °C and was associated with the degradation of hemicellulose, pectin, lignin, and cellulose (Abdullah *et al*. 2010). The DTG curves of raw EFB and raw SCB showed a shoulder at around 282 °C and 303 °C, which corresponded to pectin and hemicellulose degradation (Fig. 6b). However, the shoulder disappeared in the MCs, as the amorphous constituents were removed by chemical treatments during MC isolation. The DTG peaks from 320 to 350 °C in the MC-EFB, MC-SCB, and MC-Sigma samples represented the pyrolysis of cellulose. Theoretically, cellulose degradation results from two competing reactions, dehydration and depolymerisation (Fahma *et al*. 2010). These results agreed with those of Johar *et al.* (2012), which showed that lignocellulosic substances are composites of different kinds of components that degrade below 400 °C. Table 2 summarizes the thermal properties obtained from TGA (degradation temperature, T_{deg}) and DTG (vaporization temperature, T_{vap}, and maximum degradation temperature, T_{max}). Of the three MCs, MC-EFB had the highest thermal stability (T_{max} = 345 °C). The thermal stability of MC-EFB and MC-SCB were comparable to MC-Sigma.

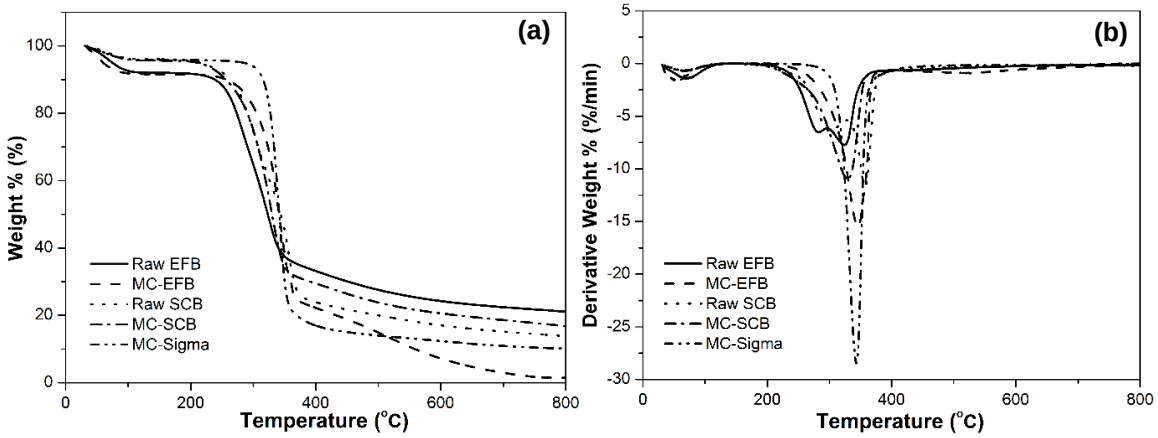

Fig. 6. (a) TGA curves and (b) DTG curves

Table 2. Thermal Properties of Raw Fibers and their MCs

Specimen	Vaporization Temperature, T_{vap} (°C)	Degradation Temperature, T_{deg} (°C)	Maximum Degradation Temperature, T_{max} (°C)
Raw EFB	71	218	325
Raw SCB	70	202	356
MC-EFB	53	256	345
MC-SCB	66	210	329
MC-Sigma	66	273	343

Differential Scanning Calorimetry

DSC curves exhibited only one clear endothermic change within the temperature range of 30 to 200 °C (Fig. 7). The endotherm that occurred from 40 to 100 °C represented the loss of water to evaporation. The moisture loss was corroborated by the TGA results. Raw EFB had the highest evaporization temperature (T_{eva}) of 55 °C, followed by raw SCB

at 54 °C. These results were attributed to hydrophilic substances such as hemicelluloses, lignin, and non-cellulosic materials that retain moisture in both raw fibers. The DSC curves of MC-EFB, MC-SCB, and MC-Sigma were found to be 50 °C, 51 °C, and 47 °C, respectively. This result is similar to the result reported by Mandal and Chakrabarty (2011). However, the cited authors studied a wider temperature range from 30 °C to 350 °C and found second endothermic changes for the raw sugarcane bagasse (161 to 241 °C) and its cellulose (253 to 290 °C), which represented the course of melting or the nature of decomposition of the crystallites. Two years later, Chan *et al*. (2013) also reported that there were two clear endothermic peaks for their kenaf core wood powder and its cellulose. They observed that the first peak for kenaf core cellulose was in the range of 32 °C to 130 °C, while the second peak was noticed at around 350 °C. Thus, the melting temperature of all the specimens in this study, especially cellulose, could not be measured by DSC since all specimens are thermally degraded at a temperature range of 200 °C to 250 °C, depending on the specimens as shown in the TGA results.

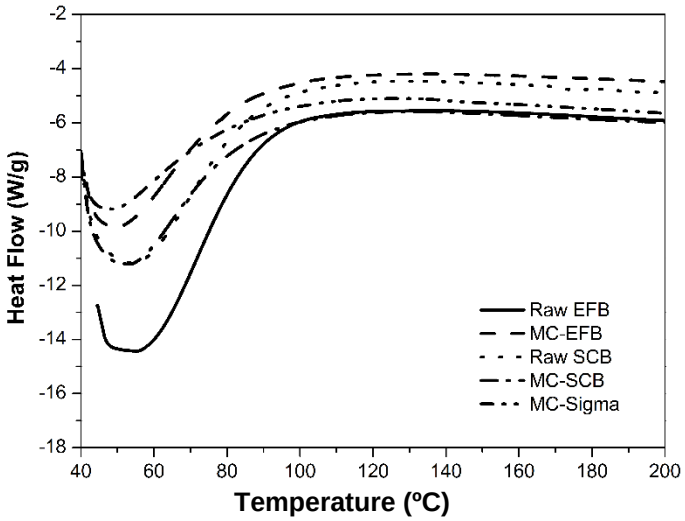

Fig. 7. DSC curves of all the specimens

CONCLUSIONS

1. Microcelluloses were chemically isolated from two different biomasses, oil palm empty fruit bunches (MC-EFB) and sugar cane bagasse (MC-SCB).
2. FTIR spectra showed that hemicellulose, lignin, and other non-cellulosic materials were removed from raw fibers by chemical treatments. XRD patterns showed that the crystallinity index of the raw fibers increased to 52.1% for MC-EFB and 52.4% for MC-SCB, but they are lower than 65.2% obtained for MC-Sigma. SEM micrographs of MCs from EFB and SCB exhibited the cellulose fibrillar structure with a smooth surface compared to MC-Sigma.
3. As revealed by TGA, the maximum degradation temperatures of MC-EFB were higher compared to MC-SCB and MC-Sigma. The DSC curves only showed the evaporation temperature of all the specimens. It was found that the T_{eva} of MC-EFB, MC-SCB and MC-Sigma were 50 °C, 51 °C, and 47 °C, respectively, indicating similarity.

4. The characteristics of MC-EFB and MC-SCB were comparable to those of the commercial MC-Sigma specimen. Therefore, EFB and SCB are promising new renewable resources for MC synthesis.

ACKNOWLEDGMENTS

The authors thank the Research Acculturation Collaborative Effort (RACE) for financial support through research grant project (9017-00005) and the Ministry of Higher Education Malaysia for the MyBrain 15 (MyMaster) Scholarship.

REFERENCES CITED

Abdul Khalil, H. P. S., Bhat, A. H., and Ireana Yusra, A. F. (2012). "Green composites from sustainable cellulose nanofibrils: A review," *Carbohydrate Polymers* 87(2), 963-979. DOI:10.1016/j.carbpol.2011.08.078.

Abdullah, S. S., Yusup, S., Ahmad, M. M., Ramli, A., and Ismail, L. (2010). "Thermogravimetry study on pyrolysis of various lignocellulosic biomass for potential hydrogen production," *Cellulose* 20, 20-42.

Abe, K., Iwamoto, S., and Yano, H. (2007). "Obtaining cellulose nanofibers with a uniform width of 15 nm from wood," *Biomacromolecules* 8(10), 3276-3278. DOI: 10.1021/bm700624p.

Adel, A. M., Abd El-Wahab, Z. H., Ibrahim, A. A., and Al-Shemy, M. T. (2011). "Characterization of microcrystalline cellulose prepared from lignocellulosic materials. Part II: Physicochemical properties," *Carbohydrate Polymers* 83(2), 676-687. DOI: 10.1016/j.carbpol.2010.08.039.

Alemdar, A., and Sain, M. (2008). "Isolation and characterization of nanofibers from agricultural residues: Wheat straw and soy hulls," *Bioresource Technology* 99(6), 1664-1671. DOI: http://dx.doi.org/10.1016/j.biortech.2007.04.029

Azeredo, H. M. C. De. (2009). "Nanocomposites for food packaging applications," *Food Research International* 42(9), 1240-1253. DOI: 10.1016/j.foodres.2009.03.019

Brinchi, L., Cotana, F., Fortunati, E., and Kenny, J. M. (2013). "Production of nanocrystalline cellulose from lignocellulosic biomass: Technology and applications," *Carbohydrate Polymers* 94(1), 154-69. DOI: 10.1016/j.carbpol.2013.01.033

Chan, C. H., Chia, C. H., Zakaria, S., Ahmad, I., and Dufresne, A. (2013). "Production and characterisation of cellulose and nano-crystalline cellulose from kenaf core wood," *BioResources* 8(1), 785-794. DOI: 10.15376/biores.8.1.785-794

Chen, J., Guan, Y., Wang, K., Zhang, X., Xu, F., and Sun, R. (2015a). "Combined effects of raw materials and solvent systems on the preparation and properties of regenerated cellulose fibers," *Carbohydrate Polymers* 128, 147-153. DOI: 10.1016/j.carbpol.2015.04.027

Chen, W., Li, Q., Cao, J., Liu, Y., Li, J., Zhang, J., Luo, S., and Yu, H. (2015b). "Revealing the structures of cellulose nanofiber bundles obtained by mechanical nanofibrillation via TEM observation," *Carbohydrate Polymers* 117, 950-956. DOI: 10.1016/j.carbpol.2014.10.024

Chen, W., Yu, H., Liu, Y., Hai, Y., Zhang, M., and Chen, P. (2011). "Isolation and characterization of cellulose nanofibers from four plant cellulose fibers using a chemical-ultrasonic process," *Cellulose* 18(2), 433-442. DOI: 10.1007/s10570-011-9497-z

Cherian, B. M., Leão, A. L., de Souza, S. F., Thomas, S., Pothan, L. A., and Kottaisamy, M. (2010). "Isolation of nanocellulose from pineapple leaf fibres by steam explosion," *Carbohydrate Polymers* 81(3), 720-725. DOI: http://dx.doi.org/10.1016/j.carbpol.2010.03.046

Das, K., Ray, D., Bandyopadhyay, N. R., and Sengupta, S. (2010). "Study of the properties of microcrystalline cellulose particles from different renewable resources by XRD, FTIR, nanoindentation, TGA, and SEM," *Journal of Polymers and the Environment* 18(3), 355-363. DOI: 10.1007/s10924-010-0167-2

De Rosa, I. M., Kenny, J. M., Puglia, D., Santulli, C., and Sarasini, F. (2010). "Morphological, thermal and mechanical characterization of okra (*Abelmoschus esculentus*) fibres as potential reinforcement in polymer composites," *Composites Science and Technology* 70(1), 116-122. DOI: 10.1016/j.compscitech.2009.09.013

Edgar, K. J., Buchanan, C. M., Debenham, J. S., Rundquist, P. A., Seiler, B. D., Shelton, M. C., and Tindall, D. (2001). "Advances in cellulose ester performance and application," *Progress in Polymer Science* 26(9), 1605-1688. DOI: 10.1016/S0079-6700(01)00027-2

Fahma, F., Iwamoto, S., Hori, N., Iwata, T., and Takemura, A. (2010). "Isolation, preparation, and characterization of nanofibers from oil palm empty-fruit-bunch (OPEFB)," *Cellulose* 17(5), 977-985. DOI: 10.1007/s10570-010-9436-4

Faruk, O., Bledzki, A. K., Fink, H.-P., and Sain, M. (2012). "Biocomposites reinforced with natural fibers: 2000-2010," *Progress in Polymer Science* 37(11), 1552–1596. DOI: 10.1016/j.progpolymsci.2012.04.003

Hamzah, F., Idris, A., and Shuan, T. K. (2011). "Preliminary study on enzymatic hydrolysis of treated oil palm (*Elaeis*) empty fruit bunches fibre (EFB) by using combination of cellulase and β 1-4 glucosidase," *Biomass and Bioenergy* 35(3), 1055-1059. DOI: 10.1016/j.biombioe.2010.11.020

Jahan, M. S., Saeed, A., He, Z., and Ni, Y. (2011). "Jute as raw material for the preparation of microcrystalline cellulose," *Cellulose* 18(2), 451-459. DOI: 10.1007/s10570-010-9481-z

Johar, N., Ahmad, I., and Dufresne, A. (2012). "Extraction, preparation, and characterization of cellulose fibres and nanocrystals from rice husk," *Industrial Crops and Products*, 37(1), 93-99. DOI: 10.1016/j.indcrop.2011.12.016

Kaushik, A., Singh, M., and Verma, G. (2010). "Green nanocomposites based on thermoplastic starch and steam exploded cellulose nanofibrils from wheat straw," *Carbohydrate Polymers* 82(2), 337-345. DOI: 10.1016/j.carbpol.2010.04.063

Kumar, A., Negi, Y. S., Bhardwaj, N. K., and Choudhary, V. (2012). "Synthesis and characterization of methylcellulose/PVA based porous composite," *Carbohydrate Polymers* 88(4), 1364-1372. DOI: http://dx.doi.org/10.1016/j.carbpol.2012.02.019

Kumar, A., Negi, Y. S., Choudhary, V., and Bhardwaj, N. K. (2014). "Characterization of cellulose nanocrystals produced by acid-hydrolysis from sugarcane bagasse as agro-waste," *Journal of Material Physics and Chemistry* 2(1), 1-8. DOI: 10.12691/jmpc-2-1-1

Laka, M., and Chernyavskaya, S. (2007). "Obtaining microcrystalline cellulose from softwood and hardwood pulp," *BioResources* 2(3), 583-589.

Lamaming, J., Hashim, R., Sulaiman, O., Leh, C. P., Sugimoto, T., and Nordin, N. A. (2015). "Cellulose nanocrystals isolated from oil palm trunk," *Carbohydrate Polymers* 127, 202-208. DOI: 10.1016/j.carbpol.2015.03.043

Le Troedec, M., Sedan, D., Peyratout, C., Bonnet, J. P., Smith, A., Guinebretiere, R., Gloaguen, V., and Krausz, P. (2008). "Influence of various chemical treatments on the composition and structure of hemp fibres," *Composites Part A: Applied Science and Manufacturing* 39(3), 514-522. DOI: 10.1016/j.compositesa.2007.12.001

Lu, T., Jiang, M., Jiang, Z., Hui, D., Wang, Z., and Zhou, Z. (2013). "Effect of surface modification of bamboo cellulose fibers on mechanical properties of cellulose/epoxy composites," *Composites Part B: Engineering* 51, 28-34. DOI: 10.1016/j.compositesb.2013.02.031

Noor Hasyierah, M. S., Zulkali, M. M. D., and Ku Syahidah, K. I. (2008). "Ferulic acid from lignocellulosic biomass: Review," in: *Proceedings of MUCET 2008 Malaysian Universities Conferences on Engineering and Technology*,Putra Brasmana, Perlis, Malaysia, pp.1-8.

Mandal, A., and Chakrabarty, D. (2011). "Isolation of nanocellulose from waste sugarcane bagasse (SCB) and its characterization," *Carbohydrate Polymers* 86(3), 1291-1299. DOI: 10.1016/j.carbpol.2011.06.030

Mikhailidi, A. M., Kotelnikova, N. E., Gensh, K. V., Kushnir, E. Y., and Bazarnova, N. G. (2014). "Composition and properties of wood and cellulose of tropical plants," *Russian Journal of Bioorganic Chemistry* 40(7), 703-713. DOI: 10.1134/S1068162014070127

Mondragon, G., Fernandes, S., Retegi, A., Peña, C., Algar, I., Eceiza, A., and Arbelaiz, A. (2014). "A common strategy to extracting cellulose nanoentities from different plants," *Industrial Crops and Products* 55, 140-148. DOI: 10.1016/j.indcrop.2014.02.014

Morais, J. P. S., Rosa, M. D. F., De Souza Filho, M. D. S. M., Nascimento, L. D., Do Nascimento, D. M., and Cassales, A. R. (2013). "Extraction and characterization of nanocellulose structures from raw cotton linter," *Carbohydrate Polymers* 91(1), 229-235. DOI: 10.1016/j.carbpol.2012.08.010

Mtibe, A., Linganiso, L. Z., Mathew, A. P., Oksman, K., John, M. J., and Anandjiwala, R. D. (2015). "A comparative study on properties of micro and nanopapers produced from cellulose and cellulose nanofibres," *Carbohydrate Polymers* 118, 1-8. DOI: 10.1016/j.carbpol.2014.10.007

Nazir, M. S., Wahjoedi, B. A., Yussof, A. W., and Abdullah, M. A. (2013). "Eco-friendly extraction and characterization of cellulose from oil palm empty fruit bunches," *BioResources* 8(2), 2161-2172. DOI: 10.15376/biores.8.2.2161-2172

Neto, W. P. F., Silvério, H. A., Dantas, N. O., and Pasquini, D. (2013). "Extraction and characterization of cellulose nanocrystals from agro-industrial residue – soy hulls," *Industrial Crops & Products* 42, 480-488. DOI: 10.1016/j.indcrop.2012.06.041

Rosa, M. F., Medeiros, E. S., Malmonge, J. A., Gregorski, K. S., Wood, D. F., Mattoso, L. H. C., Glen, G., Orts, W. J., and Imam, S. H. (2010). "Cellulose nanowhiskers from coconut husk fibers: Effect of preparation conditions on their thermal and morphological behavior," *Carbohydrate Polymers* 81(1), 83-92. DOI: 10.1016/j.carbpol.2010.01.059

Salas, C., Nypelö, T., Rodriguez-Abreu, C., Carrillo, C., and Rojas, O. J. (2014). "Nanocellulose properties and applications in colloids and interfaces," *Current*

Opinion in Colloid & Interface Science 19(5), 383-396. DOI: 10.1016/j.cocis.2014.10.003

Santos, R. M. Dos, Flauzino Neto, W. P., Silvério, H. A., Martins, D. F., Dantas, N. O., and Pasquini, D. (2013). "Cellulose nanocrystals from pineapple leaf, a new approach for the reuse of this agro-waste," *Industrial Crops and Products* 50, 707-714. DOI: 10.1016/j.indcrop.2013.08.049

Segal, L., Creely J., J., Martin E., A., and Conrad M., C. (1959). "An empirical method for estimating the degree of crystallinity of native cellulose using the X-ray diffractometer," *Textile Research Journal* 29(10), 786-794. DOI: 10.1177/004051755902901003

Sharma, A. R., Anupam, K., Swaroop, V., Lal, P. S., and Bist, V. (2015). "Pilot scale soda-anthraquinone pulping of palm oil empty fruit bunches and elemental chlorine free bleaching of resulting pulp," *Journal of Cleaner Production* 106, 422-429. DOI: 10.1016/j.jclepro.2014.03.095

Sheltami, R. M., Abdullah, I., Ahmad, I., Dufresne, A., and Kargarzadeh, H. (2012). "Extraction of cellulose nanocrystals from mengkuang leaves (*Pandanus tectorius*)," *Carbohydrate Polymers* 88(2), 772-779. DOI: 10.1016/j.carbpol.2012.01.062

Silvério, H. A., Neto, W. P. F., Dantas, N. O., and Pasquini, D. (2013). "Extraction and characterization of cellulose nanocrystals from corncob for application as reinforcing agent in nanocomposites," *Industrial Crops and Products* 44, 427-436. DOI:10.1016/j.indcrop.2012.10.014

Siqueira, G., Bras, J., and Dufresne, A. (2010). "Cellulosic bionanocomposites: A review of preparation, properties and applications," *Polymers* 2(4), 728-765. DOI: 10.3390/polym2040728

Slavutsky, A. M., and Bertuzzi, M. A. (2014). "Water barrier properties of starch films reinforced with cellulose nanocrystals obtained from sugarcane bagasse," *Carbohydrate Polymers* 110, 53-61. DOI: 10.1016/j.carbpol.2014.03.049

Tsioptsias, C., Stefopoulos, A., Kokkinomalis, I., Papadopoulou, L., and Panayiotou, C. (2008). "Development of micro-and nano-porous composite materials by processing cellulose with ionic liquids and supercritical CO_2," *Green Chemistry* 10(9), 965-971. DOI: 10.1039/B803869D

Virtanen, T., Svedström, K., Andersson, S., Tervala, L., Torkkeli, M., Knaapila, M., Kotelnikova, N., Maunu, S., and Serimaa, R. (2012). "A physico-chemical characterisation of new raw materials for microcrystalline cellulose manufacturing," *Cellulose* 19(1), 219-235. DOI: 10.1007/s10570-011-9636-6

Wang, B., Sain, M., and Oksman, K. (2007). "Study of structural morphology of hemp fiber from the micro to the nanoscale," *Applied Composite Materials* 14(2), 89-103. DOI: 10.1007/s10443-006-9032-9

Article submitted: October 2, 2015; Peer review completed: December 22, 2015; Revised version received: January 14, 2016; Accepted: January 15, 2016; Published: February 22, 2016.
DOI: 10.15376/biores.11.2.3453-3465